An Adaptive Array Excitation Scheme for the Unidirectional Enhancement of Guided Waves

Chris Adams, *Student Member, IEEE*, Sevan Harput, *Member, IEEE*, David Cowell, *Member, IEEE*, Thomas M. Carpenter, David M. Charutz, and Steven Freear, *Senior Member, IEEE*

***Abstract*— Control over the direction of wave propagation allows an engineer to spatially locate defects. When imaging with longitudinal waves, time delays can be applied to each element of a phased array transducer to steer a beam. Because of the highly dispersive nature of guided waves (GWs), this beamsteering approach is suboptimal. More appropriate time delays can be chosen to direct a GW if the dispersion relation of the material is known. Existing techniques, however, need *a priori* knowledge of material thickness and acoustic velocity, which change as a function of temperature and strain. The scheme presented here does not require prior knowledge of the dispersion relation or properties of the specimen to direct a GW. Initially, a GW is generated using a single element of an array transducer. The acquired waveforms from the remaining elements are then processed and retransmitted, constructively interfering with the wave as it travels across the spatial influence of the transducer. The scheme intrinsically compensates for the dispersion of the waves, and thus can adapt to changes in material thickness and acoustic velocity. The proposed technique is demonstrated in simulation and experimentally. Dispersion curves from either side of the array are acquired to demonstrate the scheme's ability to direct a GW in an aluminum plate. The results show that unidirectional enhancement is possible without *a priori* knowledge of the specimen using an arbitrary pitch array transducer. The experimental results show a 34-dB enhancement in one direction compared with the other.**

***Index Terms*— Bandwidth, chirp, control systems, delay effects, dispersion, energy resolution, imaging, inspection, material properties, phased arrays, signal resolution, signal to noise ratio, steel, transducers, transforms.**

I. Introduction

GUIDED waves (GWs) have been applied to a plethora of inspection problems [1], [2]. The applications are abundant and diverse. Historically, GWs have been used for the inspection of pipe work [3], [4], heat exchangers, and aging aircraft [1]. Newer aircrafts are manufactured from composites, which require sophisticated techniques for inspection [5], [6]. GWs, however, are still applicable here [7], [8]. They are widely regarded as the most promising tool for nondestructive evaluation (NDE) [9], [10] and structural health monitoring (SHM) [11]–[17]. GWs also have biomedical applications [18]–[23]. Their excellent range [9]–[11], good sensitivity [17], and flexibility of application [3], [11], [12] make them desirable in NDE and SHM.

In pipes and plates, GWs are used for detection of cracks [4], [15], delaminations [8], and corrosion. Welds [10] and joints [1], [15], [24] can be evaluated, and thickness can be measured [25]. With the correct choice of mode, which will be discussed later, GWs can propagate in pipes that are immersed or coated [1].

Lamb waves, a useful variety of GWs, are complex [1], but they are now well understood [26]–[28]. They are composed of multiple modes of oscillation [29], which is advantageous for the detection of many types of defects [3]. Low-order modes can be used for the detection of large cracks, and higher order modes can be used for the measurement of corrosion [3], [30], [31], texture, and small defects [30].

Two-dimensional Fourier analysis [14], [32] and delay-sum methods [26] can quantify the presence of modes [10]. For low frequency–thickness products, this is not problematic, as only two modes exist [9], [10], A_0 and S_0. Lamb waves are dispersive, however, so their velocity changes with frequency. At higher frequency–thickness products, low-order modes will approach Rayleigh waves, while higher order modes can have the same velocity. In SHM situations, where broadband stimulus is common place, sophisticated methods for the separation of these higher order modes exist [8]. Thus, for high-order mode inspection, it can be desirable to generate only a single mode at a time [10], [30]. Monitoring the backscatter [4] for reflections can indicate poor bonding, while mode conversions [8] can be observed when a mode interacts with the edges of a defect [14], [33]. Control over mode generation can also be useful for traversing complex materials or waveguides [34]. Mode selection, however, is not required for more common low-order mode inspection, as these modes can be easily identified.

Control over direction of propagation is advantageous to the engineer for greater range and location of defects [11], [17], [35]. With finite acoustic power, greater range can be realized by applying the wave in only one direction. Without any steering, Lamb waves will propagate in all directions equally in the waveguide. When the Lamb wave interacts with a defect, it can be difficult to locate since the reflection or mode conversion could have come from any direction. Scatter and the inherent dispersion of Lamb waves can hamper exact location of defects, but methods exist to compensate for this

Manuscript received October 18, 2016; accepted November 7, 2016. Date of publication November 11, 2016; date of current version February 1, 2017. This work was supported in part by the U.K. Engineering and Physical Sciences Research Council under Grant EP/K029835/1 and in part by the National Institute for Heart, Lung and Blood under Grant 1 U01 HL121838-01.

C. Adams, S. Harput, D. Cowell, T. M. Carpenter, and S. Freear are with the School of Electronic and Electrical Engineering, University of Leeds, Leeds, LS2 9JT, U.K. (e-mail: elca@leeds.ac.uk; s.freear@leeds.ac.uk).

D. M. Charutz is with the Soreq Nuclear Research Centre, Yavne, Israel (e-mail: dmc@soreq.gov.il).

Digital Object Identifier 10.1109/TUFFC.2016.2628100

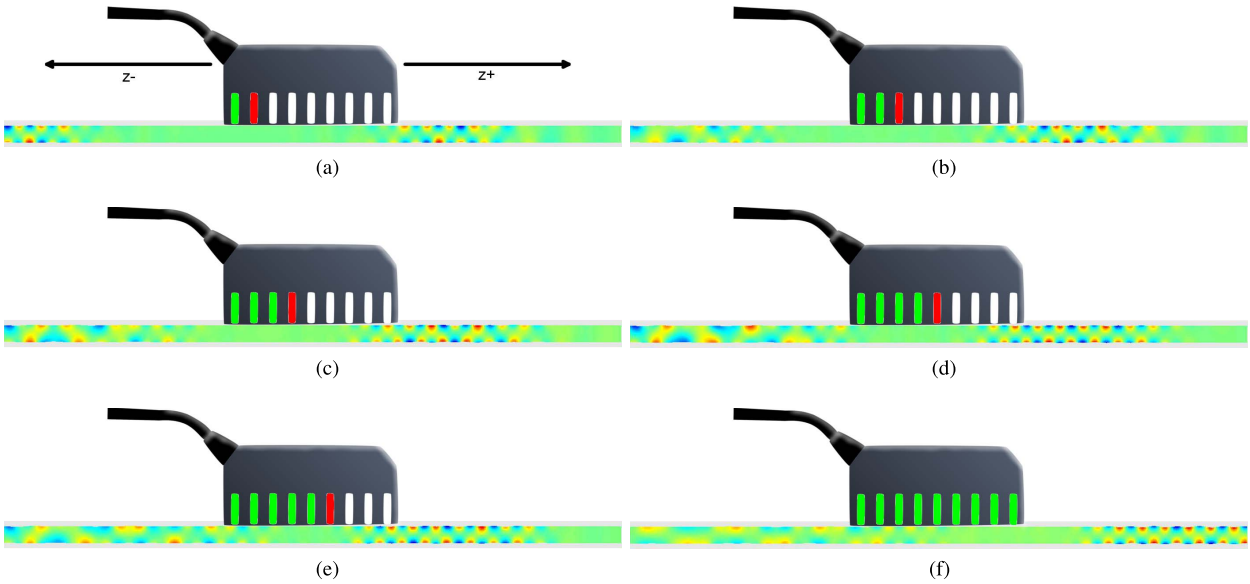

Fig. 1. Diagrammatic representation of each iteration of the scheme. A nine-element array transducer is superimposed on simulation results to show where pressure loads were applied. Elements that are highlighted in green are transmitting, while those highlighted in red are receiving. Simulation images for iterations 1–5 are captured at 17 μs. For the Nth iteration, the image was captured at 23 μs, enough time for the wave packets to exit the influence of the array. The scheme enhances GWs in one direction. (a) $i = 1$. (b) $i = 2$. (c) $i = 3$. (d) $i = 4$. (e) $i = 5$. (f) $i = N$.

[2], [16], [36]–[38]. The application of signal processing in NDE is common place [39].

While sophisticated techniques for GW inspection exist, they are not always adopted. Often not all the necessary parameters are known at the time of inspection. This is especially an issue when the specimen is placed in a harsh environment. Pipes can be under strain or be heated by their contents. In SHM, components may be exposed to extreme seasonal temperatures [40]. All these will affect the acoustic properties and dispersion relation of the material. Existing techniques are not robust to these harsh environments that may contribute to their lack of adoption. Progress is being made in the development of software to automate processes and analysis [41]. A parameter-agnostic technique for the generation of directed GWs might allow GWs to see more use in the field.

In thin plates, transmission at an oblique incidence has historically been used for control over direction, mode generation, and mode reception. Many researchers point out its limited use [11]. The engineer is limited by the angular resolution of the probe, and changing the angle can be tedious or impossible if the transducer is buried or inaccessible.

Arrays are increasingly used in NDE [42] in place of single-element transducers. Arrays can be used to excite a single mode if the pitch matches the wavelength of the desired mode. In general, arrays are favored in ultrasound because of their flexible beamforming capabilities. While beamforming of transducer arrays is often associated with medical imaging [43], these techniques are applicable to NDE also [44]. New NDE specific imaging techniques are being published too [45]. A commonly used industrial technique for creating a unidirectional array is to apply a 90° phase shift to quarter-wavelength separated elements [46]. With respect to GW specific techniques, unidirectional single-mode waves can be generated through the application of delays to each element's excitation in a phased array transducer [47]. The delays approximate the transport time of the phase for the desired mode between adjacent elements. In both cases, this is possible only with *a priori* knowledge of the specimen thickness and its dispersion curves. When the modes of the specimen are unknown, it may be possible to first obtain a dispersion curve from an edge reflector and use these results as inputs into the technique just described. However, the availability of an appropriate reflector cannot be guaranteed and it complicates an already complex inspection technique with an additional step. In SHM, authors have manufactured bonded transducers that are able to direct GWs based on the wavenumber [17].

This paper describes a scheme for the unidirectional enhancement of guided Lamb waves. The direction of propagation can be controlled without *a priori* knowledge of the material's parameters. This paper builds on existing work [48], [49] with the addition of an improved signal processing chain that has facilitated experimental validation.

II. Method

In this section, a scheme for the unidirectional enhancement of GWs is described. A short process called recursive feedback allows the scheme to resolve unknown parameters. Consisting of several short iterations, once complete, it allows unidirectional GW inspection to be undertaken. The simulation results are presented for the purpose of graphical demonstration. Following this, mathematical analysis is undertaken by comparing the scheme with an existing one. Before experimental validation can be completed, a noise filtering and truncation signal processing chain is presented. Finally, experimental process and parameters are justified.

A. Recursive Feedback

Consider a phased array transducer of N elements mounted normally on a thin plate as shown in Fig. 1.

The recursive feedback scheme is as follows.

1) $i = 1$: Initially, the first element of the transducer is excited with a linear chirp. As the first element loads the material, longitudinal and shear waves combine and create multimodal Lamb waves that travel in both directions. Simultaneously, element 2 records the surface pressure of the material.
2) $i = 2$: Now the first element transmits the same stimulus as it did before. This time, however, the second element transmits back its recording from the previous iteration. The third element records.
3) $i = 3$: In the third step of the scheme, the first element transmits its stimulus, the second its recording from step 1, and the third its recording from step 2. The fourth element records.
4) $i = N$: This process is continued until all N elements are transmitting.

The effect is that Lamb waves tend to travel in the direction of the array's spatial influence (z^+). Each element reinforces the traveling wave using its recording. Lamb waves will still propagate in the opposite direction but with less energy. The scheme will amplify forward (z^+) any modes generated by the first element.

It is often highly desirable to enhance only one mode at a time, which facilitates thorough inspection, where each mode is sensitive to different defects. However, the multimodal nature of the scheme is advantageous in two circumstances. The first is at low frequency–thickness products where the modes are easily separated by their disparate phase velocities. At this operating point, mode selection is less advantageous as modes can be very easily separated temporally. The second circumstance is the inspection of joints because the lowest order modes are most indicative of joint health. For example, complete attenuation of all modes crossing the boundary indicates a break, while a loss of the A_0 mode indicates contamination in a kissing bond joint. This process is diagrammatically shown alongside finite-element modeling (FEM) results in Fig. 1(a)–(f). In FEM, a 2.5-mm-thick aluminum sheet was used. The excitation was a 10-cycle 700–800-kHz linear chirp. Idealized pressure loads were used instead of a transducer to improve simulation efficiency, and they were separated (pitch) by 400 μm. The linear chirp was windowed with the Blackman–Harris function. In Fig. 1(a), element 1 is transmitting (green), while element 2 is recording (red). The wave packets are equal in pressure and equidistant from the first element. In Fig. 1(b), elements 1 and 2 are transmitting, and element 3 is recording. In z^+, the wave packets appear less defined than those in z^-. In Fig. 1(c), elements 1–3 are transmitting. Element 4 is recording. This process is continued until the ninth and final iteration, as shown in Fig. 1(f). Here the wave packets are most intense and well defined in z^+.

B. Background

The wavelength of a Lamb wave is described by (1). The phase velocity, C_{ph}, can be found from well-documented dispersion curves. An array transducer of pitch L can be used to amplify a particular mode. If $\lambda = L$, an excitation with a center frequency of f can be used to satisfy 1, and the corresponding mode will be amplified in both directions. This is limited of course by the pitch and bandwidth of the transducer

$$\lambda = \frac{C_{\text{ph}}}{f} \tag{1}$$

The rest of this section references work already published on the use of time delays for mode selectivity in both directions [26], [47].

For an array probe mounted to a thin waveguide, the amplitude of a generated mode is described by

$$A_{\text{m}}(z) = V \cdot F(\omega) \cdot C_{\text{m}}(z) \cdot H(\omega) \tag{2}$$

where $A_{\text{m}}(z)$ is the amplitude of mode m, V is the particle displacement, $F(\omega)$ is the frequency response of each element, and $C_{\text{m}}(z)$ is the coupling coefficient between the waveguide surface traction and the GW mode. Since the designer has no control over the coupling coefficient or the frequency response of each element, $H(\omega)$ must be changed to affect the amplitude of a mode. The following equation describes the transducer response in relation to frequency and separation when using a single frequency:

$$\begin{aligned} H(\omega) &= \sum_{i=1}^{N} e^{j[\omega t \mp \beta_m (z - z_i)]} \\ &= \frac{\sin\left(N\frac{L}{\lambda}\pi\right)}{\sin\left(\frac{L}{\lambda}\pi\right)} e^{j[\omega t \mp \beta_m (z - z_{\text{center}})]} \end{aligned} \tag{3}$$

where $\mp$ means $-$ for z^+ and $+$ for z^-, λ is the wavelength of harmonic mode m, z_{center} is the center location of the transducer array, and β is the wavenumber. To influence $H(\omega)$, either the frequency must be changed or the separation must be changed. For the designer, this is either tedious or impossible. With the introduction of an additional delay of t_{d0} to each element i, $H(\omega)$ can be influenced without changing these parameters. Consider the following equation:

$$\begin{aligned} H(\omega) &= \sum_{i=1}^{N} e^{j[\omega(t - t_i) \mp \beta_m (z - z_i)]} \\ &= \frac{\sin\left[N\pi\left(\frac{L}{\lambda} \mp \frac{t_{d0}}{T}\right)\right]}{\sin\left[\pi\left(\frac{L}{\lambda} \mp \frac{t_{d0}}{T}\right)\right]} e^{j\left[\omega\left(t - \frac{N-1}{2} t_{d0}\right) \mp \beta_m (z - z_{\text{center}})\right]}. \end{aligned} \tag{4}$$

In order to maximize the amplitude of a harmonic mode in the z^+ direction, t_{d0} should be chosen to satisfy

$$\lambda = \frac{L}{(n - t_{d0}/T)}. \tag{5}$$

T is simply $1/f$. n here is an arbitrary integer of a value that must satisfy $n > (t_{d0}/T)$. Here, t_{d0} is used to approximate the propagation time between adjacent elements, such that the peaks of the traveling mode are reinforced. It does not, however, take into consideration the dispersive nature of Lamb waves; the traveling wave will tend to temporally spread, so only one mode at one operating point is enhanced. The scheme proposed here takes this into consideration, reinforcing the traveling wave as it appears at the transducer in the previous iteration. This is key to the proposed scheme's ability to enhance multiple modes simultaneously.

C. Signal Processing

The dispersive nature of Lamb waves means that successive excitation sequences grow in length. In addition, any noise introduced by simulation artifacts or otherwise will be amplified until the experiment becomes unstable. There is a need then for signal processing to reduce the amplification of noise and to truncate the signal.

First, a bandpass filter is used to block any irrelevant frequencies, such as those that are out the frequency range of the transducer and the initial excitation. The filter must have linear phase, so a finite-impulse response design has been employed.

Recordings are then cross correlated with the initial stimulus to find the point t_0. t_0 is the lead, τ applied to maximize the correlation of initial excitation, x, and the recording, y:

$$t_0 = \arg\max_{\tau} (x \star y)(\tau). \tag{6}$$

It is imperative that noise and crosstalk between adjacent elements are rejected. Restrictions were placed on τ:

$$2 \times t_k < \tau < \frac{i}{f_{\min}}. \tag{7}$$

Here, t_k is the propagation delay in the PZT. The signal must have propagated through the first element (t_k, known), through the material (unknown), and through the second element (t_k) before it can be considered a valid correlation. The value t_k can be obtained through a simple pulse echo experiment: with a material of known dimensions and speed of sound, error between theoretical and actual time arrival will equate to $2t_k$.

$f_{\min}$ is the start frequency of the chirp, x. The upper boundary ensures that the bottom term, $n - (t_{d0}/T)$, of 5 remains positive. $n = 1$ since $L < \lambda$.

All transmissions should be of length T_t, the length of x. Abrupt truncation of the signal could introduce high-frequency components, so windowing is applied so that a gradual reduction in amplitude is achieved as $t_0 \leftarrow t$ and $t \rightarrow (t_0 + T_t)$. A Tukey window is used here to maximize total energy in the transmission while maintaining a gradual reduction in amplitude near the edges.

Finally, gain is applied to equate the peak value of x and y. The signal processing chain can be diagrammatically observed in Fig. 2.

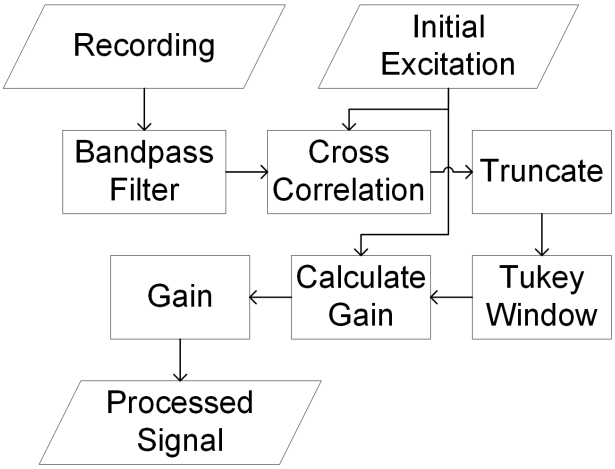

Fig. 2. Signal processing chain. The chain rejects noise and ensures that the region of interest is retransmitted.

D. Quantifying Directivity

The 2-D Fourier transform method is used to obtain a dispersion curve [32], [50]. This is accomplished by measuring the surface acoustic pressure at many points in space in monotonic intervals. Recordings are then packed together into a matrix, with dimensions of space and time. Taking the 2-D fast Fourier transform (FFT) gives a matrix of frequency against wavenumber. Since recording length and FFT size are conserved, the directivity of the scheme can be quantified by comparing the outputs of the FFTs since energy will be conserved. The peak value of the first iteration is used as a reference for power calculation.

Experimentally, several techniques exist for evaluation of surface displacement: laser vibrometers [38] and optical fibers [51] are popular choices. Here the transmitting array is used to obtain a dispersion curve for experimental simplicity. The transducer array is close to one edge and separated from the others by a much greater distance. Generated waves are reflected by the closest edge of the plate before passing over the array. It is important that the transducer is not moved between comparisons of z^+ and z^-. Repositioning the transducer might affect the coupling, and the distance to the reflecting edge cannot be reliably reproduced. To combat this, the enhancement direction of the scheme is changed while leaving the transducer *in situ*. The array is split into two. In the first experiment, z^+ is quantified by exciting toward the reflector from the middle element. In the second experiment, z^- is quantified by enhancing away from the reflector using the other half of the array. For a 64-element array, element 32 transmits during the first iteration regardless of the enhancement direction. For evaluation of z^+, elements 32–63 are energized. For evaluation of z^-, elements 32–1 are energized. Dispersion curves will be identical during the first iteration regardless of enhancement direction. This arrangement is shown in Fig. 3.

E. Experimental Parameters

Experimentally, a 64-element array probe with a pitch of 0.33 mm and center frequency of 2.5 MHz was used. The waveguide was a 0.9-mm-thick aluminum plate. A high-viscosity and high-impedance couplant is required to maximize energy transfer between the transducer and the waveguide, so a thin layer of honey is employed between the two. The transducer is placed 120 mm away from the reflecting edge and approximately 1 m from the other edges. The initial stimulus was a 10-cycle 2.25–2.75-MHz linear chirp, windowed with the Blackman–Harris function.

The first time the experiment is run, the waveforms are unknown. The received and subsequently retransmitted waveforms are related to a large number of variables relating to the material and how it disperses. The keystone of this scheme is its ability to excite modes without knowledge of the material's properties. Since the returning waveforms

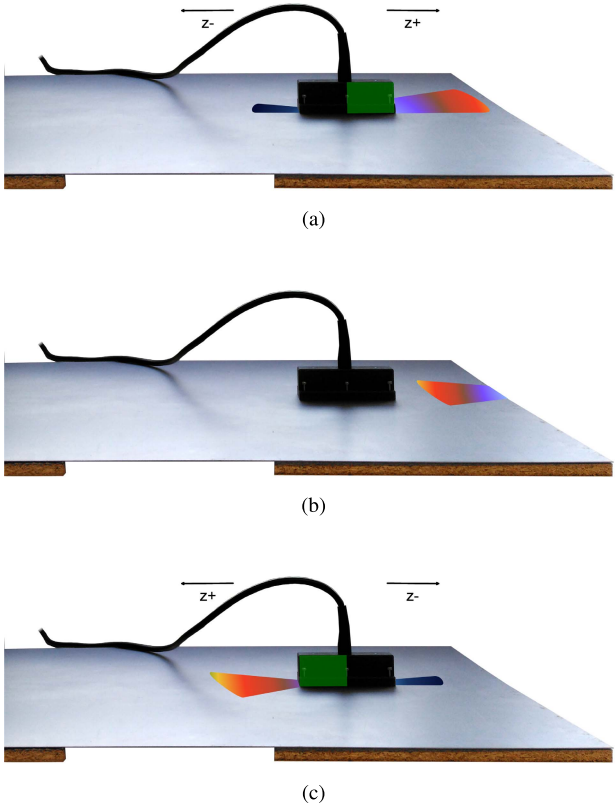

Fig. 3. Depiction of the experimental arrangement. An array transducer is mounted on a metal plate. The plate edge is used as a reflector, so that the transmitting array can also be used to acquire a dispersion curve. The array can be selectively excited to change the enhancement direction, so that both directions can be measured. Between experiments, the array is not disturbed and the first transmitting element remains the same distance from the reflector. Small pieces of wood are placed along the perimeter to acoustically isolate the plate. (a) GWs are enhanced toward the reflector. The right-hand side of the array is excited. (b) After some time, the wave packets reflect off the edge and pass over the array. The z^+ dispersion curve is acquired. (c) Enhancement direction is changed allowing the z^- dispersion curve to be obtained.

cannot possibly be predicted, arbitrary wave form generation is required. Experimentally, this was achieved using a five-level pulsewidth modulation switching scheme that provides a low total harmonic distortion [49], [52]–[57].

III. Experimental Results and Discussion

Figs. 4–6 show dispersion curves from iterations 1, 4, and 31, respectively. In each case, curves for each phase are presented. The theoretical results, which are calculated using GUIGUW [58], [59], are overlaid in white.

In the first iteration of the scheme, z^+ and z^- are almost identical, which is to be expected. In the first iteration, modes A_0, S_0, and A_1 are visible. In the fourth iteration (Fig. 5), the scheme begins to exhibit its enhancing capabilities. In the z^+ enhancement direction, there is more energy, indicated by dilation around the A_1 and S_0 modes. Fig. 6 is the last iteration in the scheme ($i = 31$). Here the enhancing capabilities of the scheme are most apparent. Compared with the first iteration, the most dominant mode in z^+, S_0, has increased by 35 dB. Modes A_0 and A_1 have increased by 30 dB. Conversely, in z^-, there is only a 10-dB increase in energy. The directional

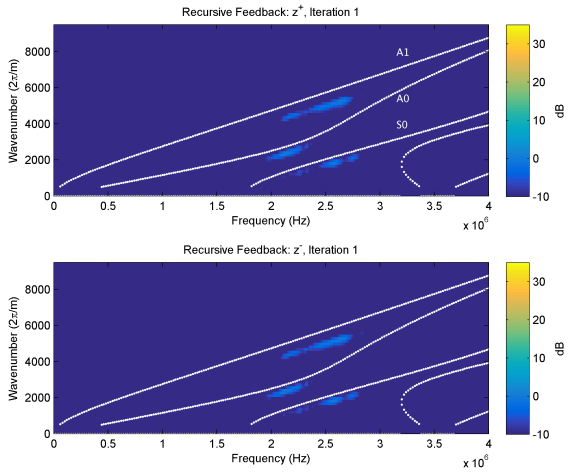

Fig. 4. Dispersion curves measured in z^+ and z^- for the first iteration. The dispersion curves are equal, and the GWs show no preference for either direction.

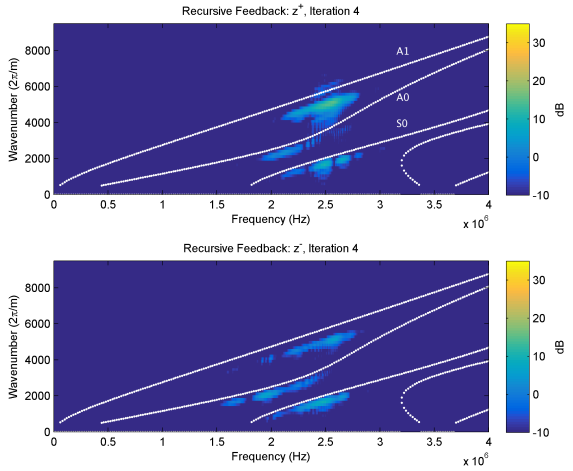

Fig. 5. Dispersion curves measured in z^+ and z^- for the fourth iteration. The scheme begins to demonstrate its steering capability.

enhancement was achieved without any knowledge of the material's dispersion curves, a requirement of other schemes.

The dispersion curves display good SNR, attributed to good coupling between transducer, honey, and waveguide. It is possible to generate Lamb waves using air coupled transducers, but mode choice is limited and the transducers are intolerant of small changes in angle [60]. In addition, an initial excitation centered around the transducer's center frequency was chosen to maximize energy in the waveguide. The dispersion curves show that most energy is between 2 and 3 MHz, as expected.

Fig. 7 shows how the amplitude ratios for each direction change with respect to frequency. For each iteration, the difference between the maximum value in z^+ and z^- at each frequency is calculated. Only the bandwidth of the chirp is considered. The green line represents the first iteration; this line is almost completely flat indicating that there is almost no difference in power in each enhancement direction. The red line represents the fourth iteration. Here, there is a peak increase of approximately 12 dB in the frequency range of the excitation. In the final iteration, which is represented by the

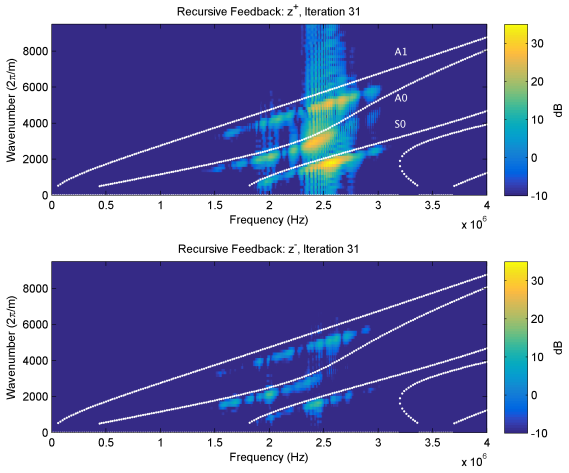

Fig. 6. Dispersion curves measured in z^+ and z^- for iteration 31. In the final iteration, the scheme shows preference for z^+ as more energy is present.

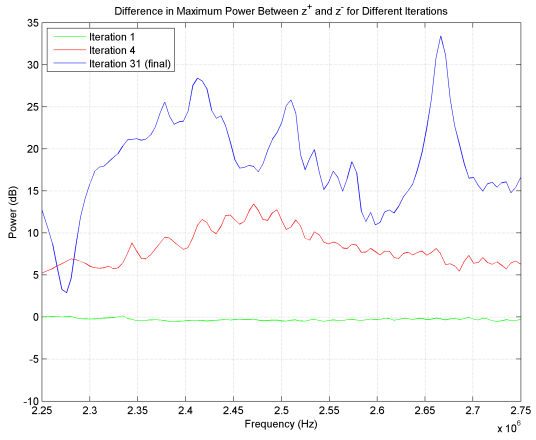

Fig. 7. Amplitude ratios between each enhancement direction are compared for iterations 1, 4, and 31. The results are given in decibels across the bandwidth of the transducer.

TABLE I
POWER DENSITIES FOR DIFFERENT ITERATIONS

Iteration	Power Density (dBHz)
1	0
4	20.96
31	51.39

blue line, the peak amplitude ratio has increased even further to a maximum of 34 dB. Although some general increase in enhancement with iteration is apparent in this graph, a better metric is power density that can be obtained through numerical integration of the linear amplitude ratios. The power densities are shown in Table I. The power reference here is the power density from the first iteration.

The choice of initial excitation will change which modes may propagate, although unlike other schemes, the scheme will enhance all valid modes. For example, a broadband impulse will excite many modes across a large frequency range. Conversely, with a narrowband linear chirp, only modes with a noninfinite velocity in the frequency range of the linear chirp can be observed. While the designer is still in the process of finalizing experimental parameters, it can be desirable to use a broadband linear chirp to increase the chances of exciting a mode, or to excite multiple modes. However, it should be noted that using a broadband signal reduces temporal resolution [61] of defects. The choice of initial excitation is critical to the success of the scheme. Experimentally and in simulation, a very narrow chirp has been used for the initial excitation in the scheme. The use of a chirp facilitates pulse compression, which allows the signal processing chain to approximate the transport time of the GWs between elements. For these reasons, impulse excitations are not appropriate as they cannot be resolved in a bandwidth limited system. The higher the time bandwidth (TB) product, the more accurate the approximation of the delay. However, the bandwidth factor is limited by the transducer. Thus, the length of the excitation must be increased, which in turn reduces resolution. Conversely, a reduction in the excitation length means that less energy can propagate in the waveguide and TB is reduced. A balance must be struck. Despite this, the reduced power budget available when undertaking remote NDT inspections will likely have the biggest influence on choice of excitation. Approximately 2-kW RMS power is required during firing using the experimental parameters given here. It may be difficult to direct the waves in materials that are either extremely thin or thick. This is because for a given frequency, f, wavelength, λ, decreases, and the scheme presumes that $L < \lambda$. Since only low-order modes are being generated, there is no risk of the GWs interacting with micro defects. Since $L < \lambda/2$, the array meets the spatial Nyquist limit and simplifies the experimental arrangement.

Lamb waves can exist in rods, thin plates [9], and cylinders, where the boundaries are in close proximity [27]. When the surface is loaded, Lamb waves form, which are the superposition of bulk and longitudinal waves [27], [62]. Lasers [63], EMATs [11], and ultrasound transducers can all be used to generate Lamb waves. EMATs are often the preferred source for buried pipes and where source influence is undesirable. Large bonded PVDF and PZT 2-D apparatus are usually used in SHM [13], [16], [31], [35], [36], [64]–[66]. Bonded PVDF is sometimes preferred in SHM because of its low cost and low source influence [14]. PZT that can be bonded to curved surfaces [67] has shown great range however [68], [69]. PZT ultrasound transducers have more source influence, but this is already understood [1]. Moveable PZT transducers arrays are more commonly used for the inspection of plates [12] and pipes [4]. Single-crystal materials look promising, which might enable generation of very long range GWs [70].

When using an array transducer, a couplant is usually required for proper transduction. The choice of couplant is often dictated by the application, and thus the scheme has been tested with various couplants to assess its robustness to different environments. Couplants of oil, water, and no couplant (air) have been tested in simulation. Dispersion curves measured for oil and water in each enhancement direction are shown in Fig. 8. The same simulation parameters have been used as in Fig. 1; however, only seven iterations of the scheme have been executed to conquer the increased simulation time incurred modeling the air. In addition, a $\lambda/4$ matching layer and a $\lambda/8$ thick wear plate have been included in the simulation. Oil

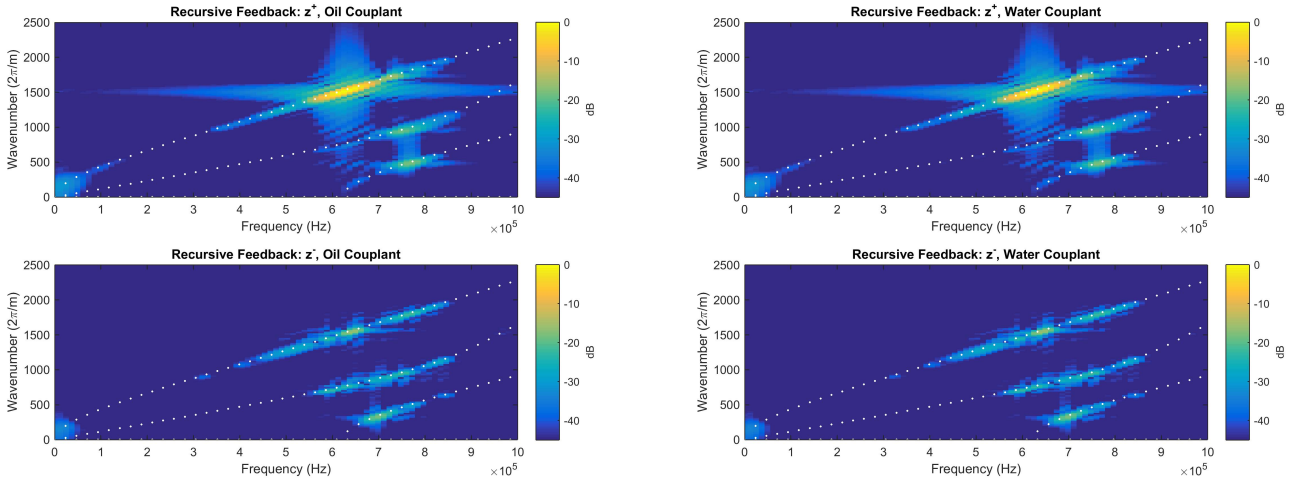

(a) (b)

Fig. 8. Couplant is usually required to maximize transduction into the waveguide. Different couplants are compared in simulation to test the scheme's robustness. Oil and water couplants work well to enhance the GWs. (a) Oil couplant. (b) Water couplant.

and water behave almost identically, with 15.6- and 15.5-dB peak enhancement achieved with each couplant, respectively. This can be attributed to their similar acoustic impedances. Using no couplant performed extremely poorly, only very low frequency components of the windowing function coupled into the waveguide and no enhancement was apparent. The peak value from the enhanced direction of each couplant is used as a power reference.

As with any contact ultrasonic experiment, the influence of the transducer can affect the results. There are two particular nuances of this experiment, which are noteworthy. First is the effect of loading applied to the transducer. Presuming that the contact area for each element in the array is far smaller than the wavelength of mode m, the coupling coefficient between the waveguide and the array element is [47]

$$C_m(z) = S * \frac{V_m^* \cdot T \cdot \hat{k}}{4P_{\text{mm}}} e^{-i\beta_m(z-z_0)} \tag{8}$$

where S is the area that the given element contacts the waveguide, V_m is the particle displacement distribution, T is the surface traction, and P_{mm} is the power density. When considering 2, it can be seen that the amplitude of a generated mode will change with surface traction. The significance of this is that as source loading is increased, modes with a wider particle displacement distribution will increase in magnitude more than modes with a narrow displacement. For this reason, pressure applied to the transducer should be carefully considered when comparing the magnitudes of modes.

The second noteworthy influence of the transducer is particular to the recursive feedback scheme. The scheme reinforces modes as they are presented to the transducer. It is possible that under the correct conditions, modes of the system may be reinforced rather than only of the waveguide. If the transducer is modeled as a single mass on top of the waveguide, then damping may occur. More significantly, individual matching and wear plate layers may incur the creation of waves not dissimilar to multilayer modes. Fortunately, a typical $\lambda/4$ thick matching layer is thin compared with the waveguide, and thus when separated by a wear plate, couplant is likely to have a small influence on the experiment. Any system modes will likely convert to single-layer plate modes at the boundaries of the transducer. The bounds applied to the cross-correlation algorithm in 7 attempt to further discourage this, as acoustic energy that has not traveled twice through the nonactive layers of the transducer is temporally discriminated. Observations from simulations that include these layers confirm this. Finally, since the experimental results are free from spurious modes and align well with the theoretical results, it can be concluded that plate modes have been enhanced as opposed to system modes when the given experimental parameters are used.

IV. Conclusion

GWs have many biomedical, NDT, and SHM applications. Their versatility makes them attractive in all these fields. While Lamb waves are complex, they are well understood, which has opened the door for research into their generation to be undertaken. They consist of many modes of oscillation, where each mode can be used for the inspection of different types of defects. While broadband sources can generate many modes, the dispersion of Lamb waves makes identification of the higher order modes more difficult because their phase velocities intersect. For low-order mode inspection, however, this is not problematic. Control over direction is desirable as it allows localization of defects, although some processing is required to compensate for the dispersion if accurate location is required. While beamforming techniques do exist for the directional enhancement of GWs, they require knowledge of the thickness of the specimen and its dispersion curves, which may be inaccessible to the operator. Arrays have been applied to solve this problem.

A scheme was devised for the unidirectional enhancement of Lamb waves. It requires no knowledge of the material's dispersion curves. In the scheme, the first element of the array generates multimodal Lamb waves in the waveguide.

The adjacent element records the Lamb wave. In the next iteration, the recording is played back. The process is repeated until all elements are transmitting. In the several short iterations, the scheme can quickly resolve parameters required for direction enhanced GW inspection. An existing scheme was reviewed, and similarities and differences between the two were discussed. Based on equations relating to the first scheme, a signal processing chain was devised to facilitate experimental validation. The signal processing chain consists of frequency filtering, cross correlation, and windowing. The chain is simple, and although difficult to implement with simple electronics, it can be easily achieved with software signal processing. Since no part of the scheme is real time, the computational requirements are minimal. On a high-end desktop computer (Intel XEON E5-1620 and 64-GB RAM), each iteration takes approximately 500 ms to process including firing. Thus, with a 32-element transducer, full 32 iterations can be executed in approximately 16 s. Most of this time, however, constitutes uploading TX waveforms to the Ultrasound Array Research Platform II. Approximately 1-GB of memory was required. There is a plenty of scope for optimization. From this point onward, GW inspection can be undertaken freely as excitations appropriate for the waveguide and transducer have been found. If the waveguide or transducer is changed, the scheme will of course need to be re-executed. As the results indicate, the more elements used the better the power density and enhancement. The number of elements used, however, is limited by the number in the array and the available computation time for deriving the waveforms for inspection.

This paper shows that it is possible to control the direction of Lamb waves using an array transducer. The strategy described within does not need any *a priori* knowledge of the material and is able to excite multiple modes while directing the GWs. In situations where the thickness or velocity of the specimen is not known, it is now possible to direct GWs for location of defects and to maximize inspection distance. The focus has been on the directional enhancement of low-order modes, which can be easily separated with Fourier analysis. Higher order modes, which are used for inspection of small defects, are harder to separate with Fourier analysis because of their intersecting phase velocities.

To quantify the directivity of the scheme, dispersion curves of the stimulated waveguide were needed. Several measurement techniques were discussed. Ultimately, the transmitting array is used in conjunction with a reflecting edge to acquire a dispersion curve. To avoid disrupting the transducer, the enhancement direction of the scheme is changed between iterations with the middle element of the array used for the first iteration. This means that the first excited element in each enhancement direction lies the same distance from the reflecting edge. The 2-D Fourier transform is applied to a time–space domain matrix to achieve a frequency–wavenumber dispersion plot. By conserving recording time, FFT size, and physical position, FFT output can be compared to demonstrate the ability of the scheme to enhance Lamb waves in one direction. The peak value from the first iteration is used as a power reference.

The scheme is first demonstrated in simulation where increased deformation is visible in the direction of the array's spatial influence. This is further verified experimentally where the effect of unidirectional enhancement becomes apparent in iteration 4. Each successive iteration shows an increase in energy in the positive enhancement direction compared with the first iteration. When all elements are transmitting during iteration 31, an increase of 34 dB is observed in z^+, where only a 10-dB increase is observed in z^- compared with energy from a single element. The amplitude ratios between enhancement directions were compared for several iterations across the bandwidth of the chirp. Following numerical integration of these data, it was shown that the power density increased between iterations.

Returning to simulation, several couplants were tested to verify the robustness of the scheme as couplant choice is often dictated by the inspection environment. A wear plate and matching layer were included in the simulation, and it was shown that oil and water performed well, achieving a 13-dB enhancement over seven iterations. Under the same operating conditions, however, air performed extremely poorly exhibiting no directional enhancement and coupling of only the lowest frequency components of the excitation occurred.

The source influence of the transducer was discussed as it may reduce the effectiveness of the scheme. It is possible that the scheme could reinforce modes of the system rather than of the plate alone. This was not observed in simulation or experimentally. With the addition of analysis, it was shown that the traction applied to the transducer may change the amplitude of individual modes.

Further research might involve 2-D directional enhancement with the use of a multidimensional array transducer. In addition, mode control, which could be achieved through dispersion reversal, might make the scheme appropriate at higher frequency–thickness products where modes cannot be separated as easily during inspection. Changes to input stimulus and additional boundaries applied to 6 might be required to achieve this.

REFERENCES

[1] J. L. Rose, "Recent advances in guided wave NDE," in *Proc. IEEE Ultrason. Symp.*, Nov. 1995, pp. 761–770.

[2] K. Xu, D. Ta, B. Hu, P. Laugier, and W. Wang, "Wideband dispersion reversal of Lamb waves," *IEEE Trans. Ultrason., Ferroelect., Freq. Control*, vol. 61, no. 6, pp. 997–1005, Jun. 2014.

[3] M. J. S. Lowe, D. N. Alleyne, and P. Cawley, "Defect detection in pipes using guided waves," *Ultrasonics*, vol. 36, nos. 1–5, pp. 147–154, Feb. 1998.

[4] J. Davies and P. Cawley, "The application of synthetic focusing for imaging crack-like defects in pipelines using guided waves," *IEEE Trans. Ultrason., Ferroelect., Freq. Control*, vol. 56, no. 4, pp. 759–771, Apr. 2009.

[5] I. Pelivanov, A. Shtokolov, C.-W. Wei, and M. O'Donnell, "A 1 kHz A-scan rate pump-probe laser-ultrasound system for robust inspection of composites," *IEEE Trans. Ultrason., Ferroelect., Freq. Control*, vol. 62, no. 9, pp. 1696–1703, Sep. 2015.

[6] A. K. Edwards, S. Savage, P. L. Hungler, and T. W. Krause, "Examination of F/A-18 honeycomb composite rudders for disbond due to water using through-transmission ultrasonics," *Ultrasound*, vol. 66, no. 2, pp. 36–44, 2011.

[7] J. L. Rose, "A baseline and vision of ultrasonic guided wave inspection potential," *J. Pressure Vessel Technol.*, vol. 124, no. 3, pp. 273–282, Jul. 2002.

[8] T. E. Michaels, J. E. Michaels, and M. Ruzzene, "Frequency–wavenumber domain analysis of guided wavefields," *Ultrasonics*, vol. 51, no. 4, pp. 452–466, May 2011.

[9] P. Cawley and D. Alleyne, "The use of Lamb waves for the long range inspection of large structures," *Proc. Ultrason. Int.*, vol. 34, nos. 2–5, pp. 287–290, Jun. 1996.

[10] D. N. Alleyne and P. Cawley, "Optimization of Lamb wave inspection techniques," *NDT E Int.*, vol. 25, no. 1, pp. 11–22, 1992.

[11] P. D. Wilcox, M. J. S. Lowe, and P. Cawley, "Mode and transducer selection for long range Lamb wave inspection," *J. Intell. Mater. Syst. Struct.*, vol. 12, no. 8, pp. 553–565, 2001.

[12] S. Fateri, P. S. Lowe, B. Engineer, and N. V. Boulgouris, "Investigation of ultrasonic guided waves interacting with piezoelectric transducers," *IEEE Sensors J.*, vol. 15, no. 8, pp. 4319–4328, Aug. 2015.

[13] A. J. Croxford, P. D. Wilcox, B. W. Drinkwater, and G. Konstantinidis, "Strategies for guided-wave structural health monitoring," *Proc. Roy. Soc. London A, Math., Phys. Eng. Sci.*, vol. 463, no. 2087, pp. 2961–2981, Nov. 2007.

[14] B. Ren and C. J. Lissenden, "PVDF multielement Lamb wave sensor for structural health monitoring," *IEEE Trans. Ultrason., Ferroelect., Freq. Control*, vol. 63, no. 1, pp. 178–185, Jan. 2016.

[15] J.-B. Ihn and F.-K. Chang, "Detection and monitoring of hidden fatigue crack growth using a built-in piezoelectric sensor/actuator network: II. Validation using riveted joints and repair patches," *Smart Mater. Struct.*, vol. 13, no. 3, pp. 621–630, May 2004.

[16] A. Perelli, L. De Marchi, A. Marzani, and N. Speciale, "Acoustic emission localization in plates with dispersion and reverberations using sparse PZT sensors in passive mode," *Smart Mater. Struct.*, vol. 21, no. 2, p. 025010, 2012.

[17] E. Baravelli, M. Senesi, M. Ruzzene, and L. De Marchi, "Fabrication and characterization of a wavenumber-spiral frequency-steerable acoustic transducer for source localization in plate structures," *IEEE Trans. Instrum. Meas.*, vol. 62, no. 8, pp. 2197–2204, Aug. 2013.

[18] A. Mahmoud *et al.*, "Noninvasive assessment of human jawbone using ultrasonic guided waves," *IEEE Trans. Ultrason., Ferroelect., Freq. Control*, vol. 55, no. 6, pp. 1316–1327, Jun. 2008.

[19] V. C. Protopappas, D. I. Fotiadis, and K. N. Malizos, "Guided ultrasound wave propagation in intact and healing long bones," *Ultrasound Med. Biol.*, vol. 32, no. 5, pp. 693–708, May 2006.

[20] J. Foiret, J. G. Minonzio, C. Chappard, M. Talmant, and P. Laugier, "Combined estimation of thickness and velocities using ultrasound guided waves: A pioneering study on *in vitro* cortical bone samples," *IEEE Trans. Ultrason., Ferroelect., Freq. Control*, vol. 61, no. 9, pp. 1478–1488, Sep. 2014.

[21] A. Mahmoud *et al.*, "P5A-10 assessment of human jawbone using ultrasonic guided wave: *In vitro* study," in *Proc. IEEE Ultrason. Symp.*, Oct. 2007, pp. 2183–2186.

[22] P. Moilanen, P. H. F. Nicholson, V. Kilappa, S. Cheng, and J. Timonen, "Assessment of the cortical bone thickness using ultrasonic guided waves: Modelling and *in vitro* study," *Ultrasound Med. Biol.*, vol. 33, no. 2, pp. 254–262, Feb. 2007.

[23] E. Maksuti, E. Widman, D. Larsson, M. W. Urban, M. Larsson, and A. Bjällmark, "Arterial stiffness estimation by shear wave elastography: Validation in phantoms with mechanical testing," *Ultrasound Med. Biol.*, vol. 42, no. 1, pp. 308–321, Oct. 2016.

[24] M. J. S. Lowe, R. E. Challis, and C. W. Chan, "The transmission of Lamb waves across adhesively bonded lap joints," *J. Acoust. Soc. Amer.*, vol. 107, no. 3, pp. 1333–1345, 2000.

[25] E. Moreno and P. Acevedo, "Thickness measurement in composite materials using Lamb waves," *Ultrasonics*, vol. 35, no. 8, pp. 581–586, Jan. 1998.

[26] W. Zhu and J. L. Rose, "Lamb wave generation and reception with time-delay periodic linear arrays: A BEM simulation and experimental study," *IEEE Trans. Ultrason., Ferroelect., Freq. Control*, vol. 46, no. 3, pp. 654–664, May 1999.

[27] J. L. Rose, *Ultrasonic Waves Solid Media*. Cambridge, U.K.: Cambridge Univ. Press, 1999.

[28] V. Dayal and V. K. Kinra, "Leaky Lamb waves in an anisotropic plate. I: An exact solution and experiments," *J. Acoust. Soc. Amer.*, vol. 85, no. 6, pp. 2268–2276, 1989.

[29] J. L. Rose, "Guided wave nuances for ultrasonic nondestructive evaluation," *IEEE Trans. Ultrason., Ferroelect., Freq. Control*, vol. 47, no. 3, pp. 575–583, May 2000.

[30] P. Khalili and P. Cawley, "Excitation of single-mode Lamb waves at high-frequency-thickness products," *IEEE Trans. Ultrason., Ferroelect., Freq. Control*, vol. 63, no. 2, pp. 303–312, Feb. 2016.

[31] P. Fromme, P. D. Wilcox, M. J. S. Lowe, and P. Cawley, "On the development and testing of a guided ultrasonic wave array for structural integrity monitoring," *IEEE Trans. Ultrason., Ferroelect., Freq. Control*, vol. 53, no. 4, pp. 777–785, Apr. 2006.

[32] D. Alleyne and P. Cawley, "A two-dimensional Fourier transform method for the measurement of propagating multimode signals," *J. Acoust. Soc. Amer.*, vol. 89, no. 3, pp. 1159–1168, 1991.

[33] Y. Cho and J. L. Rose, "A boundary element solution for a mode conversion study on the edge reflection of Lamb waves," *J. Acoust. Soc. Amer.*, vol. 99, no. 4, pp. 2097–2109, 1996.

[34] O. Asfar, B. Morvan, and J. L. Izbicki, "Three-mode coupling of symmetric and antisymmetric Lamb waves in plates with finite corrugations," *IEEE Trans. Ultrason., Ferroelect., Freq. Control*, vol. 62, no. 3, pp. 524–530, Mar. 2015.

[35] P. S. Tua, S. T. Quek, and Q. Wang, "Detection of cracks in plates using piezo-actuated Lamb waves," *Smart Mater. Struct.*, vol. 13, no. 4, p. 643, May 2004.

[36] J. E. Michaels, A. J. Croxford, and P. D. Wilcox, "Imaging algorithms for locating damage via *in situ* ultrasonic sensors," in *Proc. IEEE Sensors Appl. Symp. (SAS)*, Feb. 2008, pp. 63–67.

[37] S. Fu, L. Shi, Y. Zhou, and J. Cai, "Dispersion compensation in Lamb wave defect detection with step-pulse excitation and warped frequency transform," *IEEE Trans. Ultrason., Ferroelect., Freq. Control*, vol. 61, no. 12, pp. 2075–2088, Dec. 2014.

[38] X. Chen, J. E. Michaels, and T. E. Michaels, "A methodology for estimating guided wave scattering patterns from sparse transducer array measurements," *IEEE Trans. Ultrason., Ferroelect., Freq. Control*, vol. 62, no. 1, pp. 208–219, Jan. 2015.

[39] Y. Lu and J. Saniie, "Adaptive filtering and Fractional Fourier transform for ultrasonic signal processsing and flaw detection," in *Proc. IEEE Int. Ultrason. Symp.*, Sep. 2014, pp. 1932–1935.

[40] G. Konstantinidis, P. D. Wilcox, and B. W. Drinkwater, "An investigation into the temperature stability of a guided wave structural health monitoring system using permanently attached sensors," *IEEE Sensors J.*, vol. 7, no. 5, pp. 905–912, May 2007.

[41] J. Bingham and M. Hinders, "Lamb wave detection of delaminations in large diameter pipe coatings," *Open Acoust. J.*, vol. 2, pp. 75–86, Nov. 2009.

[42] B. W. Drinkwater and P. D. Wilcox, "Ultrasonic arrays for non-destructive evaluation: A review," *NDT E Int.*, vol. 39, no. 7, pp. 525–541, Oct. 2006.

[43] K. K. Shung, M. B. Smith, and B. M. W. Tsui, *Principles of Medical Imaging*. San Diego, CA, USA: Academic, 1992.

[44] L. Moreau, B. W. Drinkwater, and P. D. Wilcox, "Ultrasonic imaging algorithms with limited transmission cycles for rapid nondestructive evaluation," *IEEE Trans. Ultrason., Ferroelect., Freq. Control*, vol. 56, no. 9, pp. 1932–1944, Sep. 2009.

[45] J. Zhang, B. W. Drinkwater, P. D. Wilcox, and A. J. Hunter, "Defect detection using ultrasonic arrays: The multi-mode total focusing method," *NDT E Int.*, vol. 43, no. 2, pp. 123–133, Mar. 2010.

[46] C. Vasile and F. Carmine, "Periodic magnet unidirectional transducer," U.S. Patent 4 232 557, Nov. 11, 1980.

[47] J. Li and J. L. Rose, "Implementing guided wave mode control by use of a phased transducer array," *IEEE Trans. Ultrason., Ferroelect., Freq. Control*, vol. 48, no. 3, pp. 761–768, May 2001.

[48] C. Adams, S. Harput, D. M. J. Cowell, S. Freear, and D. M. Charutz, "Specimen-agnostic guided wave inspection using recursive feedback," in *Proc. IEEE Int. Ultrason. Symp. (IUS)*, Sep. 2016, pp. 1–4.

[49] D. M. Charutz, E. Mor, S. Harput, D. M. J. Cowell, P. Smith, and S. Freear, "Guided wave enhancement phased array beamforming scheme using recursive feedback," in *Proc. IEEE Int. Ultrason. Symp. (IUS)*, Jul. 2013, pp. 166–169.

[50] C. Adams, S. Harput, D. M. J. Cowell, and S. Freear, "A phase velocity filter for the measurement of Lamb wave dispersion," in *Proc. IEEE Int. Ultrason. Symp. (IUS)*, Sep. 2016, pp. 1–4.

[51] A. Gachagan *et al.*, "Generation and reception of ultrasonic guided waves in composite plates using conformable piezoelectric transmitters and optical-fiber detectors," *IEEE Trans. Ultrason., Ferroelect., Freq. Control*, vol. 46, no. 1, pp. 72–81, Jan. 1999.

[52] D. M. J. Cowell, P. Smith, S. Harput, J. McLaughlan, and S. Freear, "Non-linear harmonic reduction pulse width modulation (HRPWM) for the arbitrary control of transducer-integrated switched excitation electronics," in *Proc. IEEE Int. Ultrason. Symp.*, Sep. 2014, pp. 807–810.

[53] D. M. J. Cowell, P. R. Smith, and S. Freear, "Phase-inversion-based selective harmonic elimination (PI-SHE) in multi-level switched-mode

tone–and frequency–modulated excitation," *IEEE Trans. Ultrason., Ferroelect., Freq. Control*, vol. 60, no. 6, pp. 1084–1097, Jun. 2013.
[54] P. R. Smith, D. M. J. Cowell, and S. Freear, "Width-modulated square-wave pulses for ultrasound applications," *IEEE Trans. Ultrason., Ferroelect., Freq. Control*, vol. 60, no. 11, pp. 2244–2256, Nov. 2013.
[55] R. H. Ingham, R. James, P. R. Smith, D. M. J. Cowell, and S. Freear, "Transducer excitation with switched-mode encoded signals for harmonic and amplitude control verified using the leach model," in *Proc. IEEE Int. Ultrason. Symp. (IUS)*, Jul. 2013, pp. 457–460.
[56] S. Harput, M. Arif, J. McLaughlan, D. M. J. Cowell, and S. Freear, "The effect of amplitude modulation on subharmonic imaging with chirp excitation," *IEEE Trans. Ultrason., Ferroelect., Freq. Control*, vol. 60, no. 12, pp. 2532–2544, Dec. 2013.
[57] D. M. J. Cowell, P. R. Smith, and S. Freear, "Harmonic cancellation in switched mode linear frequency modulated (LFM) excitation of ultrasound arrays," in *Proc. IEEE Int. Ultrason. Symp.*, Oct. 2011, pp. 454–457.
[58] I. Bartoli, A. Marzani, F. L. di Scalea, and E. Viola, "Modeling wave propagation in damped waveguides of arbitrary cross-section," *J. Sound Vibrat.*, vol. 295, nos. 3–5, pp. 685–707, 2006.
[59] P. Bocchini, A. Marzani, and E. Viola, "Graphical user interface for guided acoustic waves," *J. Comput. Civil Eng.*, vol. 25, no. 3, pp. 202–210, May 2011.
[60] M. Castaings and P. Cawley, "The generation, propagation, and detection of Lamb waves in plates using air-coupled ultrasonic transducers," *J. Acoust. Soc. Amer.*, vol. 100, no. 5, pp. 3070–3077, 1996.
[61] J. E. Michaels, S. J. Lee, A. J. Croxford, and P. D. Wilcox, "Chirp excitation of ultrasonic guided waves," *Ultrasonics*, vol. 53, no. 1, pp. 265–270, 2013.
[62] I. A. Viktorov, *Rayleigh and Lamb Waves: Physical Theory and Applications*. New York, NY, USA: Plenum, 1970.
[63] S. E. Burrows, B. Dutton, and S. Dixon, "Laser generation of Lamb waves for defect detection: Experimental methods and finite element modeling," *IEEE Trans. Ultrason., Ferroelect., Freq. Control*, vol. 59, no. 1, pp. 82–89, Jan. 2012.
[64] R. Levine and J. Michaels, "Block-sparse reconstruction and imaging for Lamb wave structural health monitoring," *IEEE Trans. Ultrason., Ferroelect., Freq. Control*, vol. 61, no. 6, pp. 1006–1015, Jun. 2014.
[65] J. Hall and J. Michaels, "Minimum variance ultrasonic imaging applied to an *in situ* sparse guided wave array," *IEEE Trans. Ultrason., Ferroelect., Freq. Control*, vol. 57, no. 10, pp. 2311–2323, Oct. 2010.
[66] J. B. Harley and J. M. F. Moura, "Data-driven and calibration-free Lamb wave source localization with sparse sensor arrays," *IEEE Trans. Ultrason., Ferroelect., Freq. Control*, vol. 62, no. 8, pp. 1516–1529, Aug. 2015.
[67] A. Gachagan, P. Reynolds, G. Hayward, and A. McNab, "Construction and evaluation of a new generation of flexible ultrasonic transducers," in *Proc. IEEE Ultrason. Symp.*, vol. 2. Nov. 1996, pp. 853–856.
[68] B. Hailu, G. Hayward, A. Gachagan, A. McNab, and R. Farlow, "Comparison of different piezoelectric materials for the design of embedded transducers for structural health monitoring applications," in *Proc. IEEE Ultrason. Symp.*, vol. 2. Oct. 2000, pp. 1009–1012.
[69] A. Gachagan, G. Hayward, and R. Banks, "A flexible piezoelectric transducer design for efficient generation and reception of ultrasonic Lamb waves," *IEEE Trans. Ultrason., Ferroelect., Freq. Control*, vol. 52, no. 7, pp. 1175–1182, Jul. 2005.
[70] P. Marin-Franch, S. Cochran, and K. Kirk, "Progress towards ultrasound applications of new single crystal materials," *J. Mater. Sci., Mater. Electron.*, vol. 15, no. 11, pp. 715–720, Nov. 2004.

Chris Adams (S'16) received the B.Eng degree in electronic and electrical engineering in 2013. He subsequently worked in industry for 2 years as an FPGA designer. Since 2015, he has been pursuing the Ph.D. degree with the University of Leeds, Leeds, U.K.

His doctoral studies are sponsored by UK-EPSRC. His research interests involve NDT and biomedical applications of guided waves.

Sevan Harput (S'08–M'14) received the B.Sc. degree in microelectronics engineering and the M.Sc. degree in electronic engineering and computer sciences from Sabanci University, Tuzla, Turkey, in 2005 and 2007, respectively, and the Ph.D. degree from the University of Leeds, Leeds, U.K., in 2013.

He was a Teaching and Research Fellow with Sabanci University, between 2007 and 2008. In 2009, he joined the Ultrasound Group, School of Electronic and Electrical Engineering, University of Leeds. Between 2013 and 2016, he was a Research Fellow with the University of Leeds. Currently, he is a Research Associate with the Department of Bioengineering, Imperial College London, London, U.K., and a Visiting Scholar at the University of Leeds. His current research interests include high frame-rate ultrasound imaging, super-resolution imaging, Doppler and low imaging, elastography, coded excitation techniques, nonlinear acoustics, and ultrasound contrast agents.

Dr. Harput was a recipient of the University of Leeds Teaching and Research Award in 2014. He has been an Editorial and Administrative Assistant for IEEE TRANSACTIONS ON ULTRASONICS, FERROELECTRICS, AND FREQUENCY CONTROL since 2013.

David Cowell (M'14) received the Ph.D. degree from the University of Leeds, Leeds, U.K., in 2008, for research on advanced coding techniques and excitation circuit design for industrial instrumentation and medical imaging ultrasound systems.

He performed extensive consultancy in instrumentation, field-programmable gate arrays, and high-speed digital hardware design. Following work as a Research Consultant in measurement and instrumentation, he joined the Ultrasound Group, University of Leeds, as a Research Fellow. His current research interests include noninvasive industrial ultrasound measurement and advanced miniaturized ultrasound excitation systems with low harmonic distortion for phased array imaging, ultrasound system design, and signal processing.

Thomas M. Carpenter received the M.Eng. degree in electronic and electrical engineering from the University of Leeds, Leeds, U.K., in 2014.

He joined the Georgia Institute of Technology, Atlanta, GA, USA, as a Research Engineer, where he developed high-speed field-programmable gate array (FPGA) designs for ultrasound imaging applications. He is currently a Visiting Researcher with the Ultrasound Research Group, University of Leeds. His current research interests include embedded systems and FPGA design, both in the biomedical field and for industrial applications.

David M. Charutz received the Ph.D. degree from The Hebrew University of Jerusalem, Jerusalem, Israel, in 1993, where he was involved in investigating the molecular dynamics of simple reactions in liquids.

From 1994 to 1995, he was a Post-Doctoral Research Assistant with the Chemistry and Biochemistry Department, University of California at Los Angeles, Los Angeles, CA, USA, where he developed molecular electronic structure algorithms based on a statistical approach. He joined SOREQ Nuclear Research Center, Yavne, Israel, where he serves until today as a Researcher. In 2004, he joined the Ultrasonic Group, NDT Department, SOREQ, where he was involved in developing NDT ultrasonic phased-array-based techniques and methods to identify and allocate cracks and flaws in various solid objects. In 2011, he became the Head of the Ultrasonic Group in his institute. In 2012, he was on sabbatical leave, working in collaboration with the University of Leeds, Leeds, U.K., Ultrasonic Group. He worked on a phased array guided wave amplification method to be utilized in industrial NDT systems. Since 2013, he returned to his position in SOREQ.

Steven Freear (S'95–M'97–SM'11) received the doctorate degree in 1997 and subsequently worked in the electronics industry for 7 years as a medical ultrasonic system designer. He was appointed Lecturer (Assistant Professor), Senior Lecturer (Associate Professor), and then Professor in 2006, 2008, and 2016, respectively, at the School of Electronic and Electrical Engineering at the University of Leeds, Leeds, U.K. In 2006, he formed the Ultrasound Group, specializing in both industrial and biomedical research. His main research interest is concerned with advanced analog and digital signal processing and instrumentation for ultrasonic systems. He teaches digital signal processing, VLSI and embedded systems design, and hardware description languages at both undergraduate and postgraduate levels. He was elected Editor-in-Chief in 2013 for the IEEE TRANSACTIONS ON ULTRASONICS, FERRORELECTRICS, AND FREQUENCY CONTROL. In June 2014 he was appointed Visiting Professor at Georgia Tech. He is External Examiner to undergraduate programmes in Electronic Engineering at Queens University, Belfast.